I&EC research
Industrial & Engineering Chemistry Research

REVIEW

pubs.acs.org/IECR

Thermodynamic Properties of Uranyl Minerals: Constraints from Calorimetry and Solubility Measurements

Tatiana Y. Shvareva,[†] Jeremy B. Fein,[‡] and Alexandra Navrotsky*[,†]

[†]University of California, Davis, Peter A. Rock Thermochemistry Laboratory, One Shields Avenue, Davis, California 95616, United States

[‡]University of Notre Dame, Department of Civil Engineering and Geological Sciences, 156 Fitzpatrick Hall, Notre Dame, Indiana 46556, United States

ABSTRACT: More than 50 uranyl minerals, phases containing U^{6+} as the uranyl UO_2^{2+} cation, and hydroxide, carbonate, phosphate, and silicate anions, H_2O, and alkali and alkaline earth cations, occur in nature and as corrosion products of spent nuclear fuel. Despite their importance and the need to understand their thermodynamics to predict uranium solubility, fate, and transport in the environment, reliable thermodynamic data have only been available recently. This paper summarizes recent studies of enthalpies of formation using high temperature oxide melt solution calorimetry and Gibbs free energies from solubility experiments. Standard state thermochemical parameters (at 25 °C and 1 bar) are tabulated and the stability and transformation sequences of these phases are discussed. The enthalpies of formation from oxides are discussed in terms of crystal structure and Lewis acid−base interactions.

INTRODUCTION

As nuclear power becomes an increasing source of world energy, the environmental fate of actinides must be unambiguously predicted. Because, in the long term, spent nuclear fuel is not stable under moist oxidizing conditions, oxidative dissolution of radionuclides in groundwater with consequent formation of uranyl minerals is a likely alteration pathway.[1−3] With uraninite (UO_2) being the major component of nuclear fuel, the most crucial studies are focused on uranyl-based phases in which uranium is oxidized to the +6 state and is present as the UO_2^{2+} cation. Numerous tests of natural analogs[1,4−6] and synthesized samples (for example 2,7,8) on alteration of UO_2 reveal uranyl oxide hydrate minerals and uranyl silicates as major products. Also, uranyl phosphates and carbonates can be formed under some groundwater compositions.[5] Mineral stabilities and solubilities determine which solid phases form, and the distribution of uranium between solid and aqueous phases. Recently, it was also shown that some uranyl minerals can incorporate Pu and Np into their structures, serving as host phases and thereby reducing heavy actinide mobility.[9−12] Thus, the knowledge of thermodynamic parameters for environmental actinide phases is critical for control, prevention, and remediation of radioactive contamination.

Despite such obvious need for reliable thermodynamic data for uranyl minerals, previously reported data are incomplete and somewhat contradictory. Grenthe et al.,[13] followed by Guillaumont et al.,[14] compiled and reviewed the chemical thermodynamics of actinide materials and only very few values have been accepted as reliable for hydrated crystalline uranyl oxides, carbonates, phosphates, and silicates. These uranyl minerals are complex, structurally and chemically, with more than 50 phases known,[15] and the synthesis of pure materials and their detailed characterization are not straightforward. Due to nonstoichiometry, their hydrous nature and complex oxidation−reduction behavior, the best choice of thermodynamic measurement methods is a challenge.

For example, Santalova et al.[16] reported enthalpy of formation of dihydrated (meta)schoepite $UO_3 \cdot 2H_2O$ from solution calorimetry in dilute HF as −1840.6 kJ/mol. Later, Tasker et al.[17] determined the enthalpy of formation of $UO_3 \cdot 2H_2O$ as −1825.4 ± 2.1 kJ/mol by calorimetry in more concentrated HF. There were extensive solubility measurements with different techniques on meta-schoepite that resulted in solubility products varying from 4.68 to 6.23.[18−21] Other uranyl oxide hydrates, becquerelite $Ca[(UO_2)_3O_2(OH)_3]_2 \cdot 8H_2O$, clarkeite $Na(UO_2)O(OH)$, and compregnacite $Na_2[(UO_2)_3O_2(OH)_3]_2 \cdot 7H_2O$, have not been studied directly by solution calorimetric methods. The solubility data strongly depend on the crystallinity of samples and had not been accurately determined.[22]

Thermodynamic properties of uranyl carbonates are also poorly constrained. There are several reliable solubility measurements for rutherfordine UO_2CO_3 reported,[19,20,23−25] but the enthalpy of formation, −1689.6 ± 1.8 kJ/mol, accepted by Guillaumont et al.,[14] has been calculated from averaged solubility data and an experimentally determined standard entropy S° value,[25] and not measured directly. Alwan and Williams[26] reported enthalpy and Gibbs free energy of formation for andersonite $Na_2Ca[(UO_2)(CO_3)_3] \cdot 5H_2O$ but did not report experimental conditions or details of measurements. Data on other uranyl carbonates are very limited and are restricted only to solubility estimates.[13,14]

Cordfunke et al.[27] measured the enthalpy of formation of $(UO_2)_3(PO_4)_2$ by solution calorimetry in concentrated H_2SO_4 as −5491.3 ± 3.5 kJ/mol. With entropy values measured by Barten,[28] the Gibbs free energy of formation of $(UO_2)_3(PO_4)_2$,

Special Issue: Alternative Energy Systems: Nuclear Energy

Received: February 4, 2011
Accepted: November 12, 2011
Revised: October 11, 2011
Published: November 12, 2011

Table 1. Thermodynamic Functions for Formation from Oxides and Elements of Uranyl Minerals, under Standard Temperature and Pressure

phase, formula	formula per one uranyl cation	$\Delta H_{f,\ ox}$, kJ/mol	$\Delta H_{f,\ el}$, kJ/mol	$\Delta G_{f,\ el}$, kJ/mol	$\Delta S_{f,\ el}$, J/mol·K	$S°$, J/mol·K
		uranyl oxides hydrates and peroxides				
metaschoepite $UO_3 \cdot 2H_2O$	$UO_3(H_2O)_2$	4.4 ± 3.1	−1791.0 ± 3.2	−1632.2 ± 7.4	−532.5 ± 8.1	−1356.6 ± 8.1
β-$UO_2(OH)_2$	β-$UO_2(OH)_2$	−26.6 ± 2.8	−1536.2 ± 2.8			
bequerelite $Ca[(UO_2)_3O_2(OH)_3]_2 \cdot 8H_2O$	$Ca_{0.17}(UO_2)\ O_{0.67}(OH)\ (H_2O)_{1.3}$	−44.6 ± 2.2	−1898.2 ± 2.3	−1717.6 ± 4.4	−605.8 ± 5.0	−1407.8 ± 5.0
clarkeite $Na(UO_2)O(OH)$	$Na(UO_2)O(OH)$	−150.6 ± 4.9	−1724.7 ± 5.1	−1635.1 ± 23.4	−300.5 ± 23.9	−891.0 ± 23.9
Na-compreignacite $Na_2[(UO_2)_3O_2(OH)_3]_2 \cdot 7H_2O$	$Na_{0..34}(UO_2)O_{0.67}(OH)(H_2O)_{1.2}$	−53.5 ± 2.4	−1822.7 ± 2.4	−1674.3 ± 4.1	−497.9 ± 5.0	−1286.9 ± 5.0
curite $Pb_3(UO_2)_8O_8(OH)_6 \cdot \bullet 2H_2O$	$Pb_{0.38}(UO_2)\ O\ (OH)_{0.76}(H_2O)_{0.3}$	−161.5 ± 4.3	−1645.4 ± 4.3			
studtite $(UO_2)O_2 \cdot 4H_2O$, oxide + H_2O	$(UO_2)O_2(H_2O)_4$	22.3 ± 3.9	−2344.7 ± 4.0			
studtite $(UO_2)O_2 \cdot 4H_2O$, oxide + H_2O_2		−75.7 ± 4.1				
		uranyl carbonates				
rutherfordine UO_2CO_3	UO_2CO_3	−99.1 ± 4.2	−1716.4 ± 4.2			
andersonite $Na_2Ca[(UO_2)(CO_3)_3] \cdot 5H_2O$	$Na_2Ca[(UO_2)(CO_3)_3](H_2O)_5$	−710.4 ± 9.1	−5593.6 ± 9.1			
grimselite $K_3NaUO_2(CO_3)_3 \cdot H_2O$	$K_3NaUO_2(CO_3)_3(H_2O)$	−989.3 ± 14.0	−4431.6 ± 15.3			
		uranyl phosphates				
$UO_2HPO_4 \cdot 3H_2O$	$UO_2HPO_4(H_2O)_3$	−241.0 ± 3.9	−3223.2 ± 4.0	−3072.3 ± 4.8	−1302.3 ± 21.2	−2774.1 ± 21.2
$(UO_2)_3(PO_4)_2 \cdot 4H_2O$	$UO_2(PO_4)_{2/3}(H_2O)_{4/3}$	−227.2 ± 2.3	−2333.7 ± 4.6	−2046.3 ± 12.2	−964.3 ± 6.2	−1831.6 ± 20.6
		uranyl silicates				
soddyite $(UO_2)_2(SiO_4) \cdot 2H_2O$	$(UO_2)(SiO_4)_{1/2}(H_2O)$	−117.8 ± 4.3	−2022.7 ± 2.5	−1826.1 ± 2.1	−635.4 ± 10.9	−1338.4 ± 10.9
K-boltwoodite $K(UO_2)(SiO_3OH) \cdot 1.3H_2O$	$K(UO_2)(SiO_3OH)(H_2O)$	−238.5 ± 6.0	−2768.1 ± 6.5	−2758.6 ± 3.5	−27.5 ± 7.3	−1075.0 ± 7.3
Na-boltwoodite $Na(UO_2)(SiO_3OH) \cdot H_2O$	$Na(UO_2)(SiO_3OH)(H_2O)$	−215.9 ± 6.5	−2947.2 ± 4.0	−2725.2 ± 2.6	−352.5 ± 7.2	−1386.6 ± 7.2
uranophane $Ca(UO_2)_2(SiO_3OH) \cdot 5H_2O$	$Ca_{0.5}(UO_2)\ (SiO_3OH_{0.5})(H_2O)_{2.5}$	−150.0 ± 4.3	−3399.7 ± 4.0	−3099.3 ± 5.6	−1007.6 ± 12.0	−2321.0 ± 12.2

−5116.0 ± 5.5 kJ/mol, was established. However for hydrated forms that crystallize environmentally, $(UO_2)_3(PO_4)_2 \cdot 4H_2O$ and $(UO_2)_3(PO_4)_2 \cdot 6H_2O$, only solubility was evaluated.[13,14] Another important uranyl phosphate, autunite, in its H^+ and Ca^{2+} forms (as $HUO_2PO_4 \cdot xH_2O$ and $Ca(UO_2)_2(PO_4)_2 \cdot xH_2O$, respectively), also has several crystalline hydrated forms for which some solubility measurements are reported,[14] however, they are not well constrained.[22]

The uranyl silicate group is one of the most important of the uranyl mineral family; however, it is the least studied thermodynamically. Only sparse solubility data could be found[14] and no K_{sp} values were accepted for soddyite $(UO_2)_2SiO_4 \cdot 4H_2O$, uranophane $Ca(UO_2)_2(HSiO_4)_2 \cdot 5H_2O$, or boltwoodite $K(UO_2)(HSiO_4O) \cdot H_2O$ by Guillaumont et al.[14]

Finch[29] proposed a database of calculated thermodynamic properties of uranyl minerals based on Gibbs free energies of formation estimated as a simple arithmetic sum of energetic contributions from constituent oxides. Chen et al.[30] suggested a method of summarizing molar contributions from structural components of the crystalline material. Using an assumption that particular coordination polyhedra make similar energetic contributions to all minerals, Chen et al. created a database for minerals whose structures had been explicitly determined. However materials with unusual or distorted structures, as well as with structures with abnormally strong or weak bonding between structural units, were not included.

Thus, there is an urgent need to develop a comprehensive thermodynamic database for uranyl minerals that is consistent with the experimental data. Recently, high temperature oxide melt solution calorimetry combined with solubility measurements approaching equilibrium from both supersaturated and undersaturated conditions have been employed for thermodynamic characterization of uranyl species.[31−34] Summary of measured data (Table 1) leads to systematics and comparison with predicted values for uranyl oxide hydrates, carbonates, phosphates, and silicates, and is the primary focus of the current review.

DISCUSSION

Enthalpy of Formation from Oxides and Elements. High temperature oxide melt solution calorimetry is advantageous over other techniques for enthalpy measurements of uranyl minerals. The high temperature of the solvent (700 °C) facilitates complete dissolution of uranyl materials regardless of their structure and composition. Drop mode of experiments, in which the sample is dropped from room temperature directly into the solvent, eliminates any sample decomposition at high temperature prior to the reaction in the calorimeter. The measured heat effect is the sum of heat capacity and enthalpy of solution in the calorimetric solvent.[35,36] Enthalpy of formation at room temperature can be calculated from these data through well-defined thermodynamic cycles referred to the corresponding binary oxides and elements. Table 2 represents an example of a thermodynamic cycle used to calculate enthalpies of formation of soddyite $(UO_2)_2(SiO_4) \cdot 2H_2O$.[33]

A custom-built Calvet microcalorimeter with twin design has been used for enthalpy measurements.[35,36] The high sensitivity of this instrument permits measurements on exceptionally small amounts of sample (5 mg per drop), so not more than 50 mg is needed to collect a complete data set. A version of this calorimeter is now commercially available.

The calorimeter is calibrated against the well-known heat content of Al_2O_3. Prior to each experiment, the complete dissolution of the mineral in $3Na_2O \cdot 4MoO_3$ has been confirmed by experiments in a furnace. For calorimetry on uranyl silicates, the final state of silica was experimentally identified as cristobalite.[33]

dx.doi.org/10.1021/ie2002582 |Ind. Eng. Chem. Res. 2012, 51, 607–613

Table 2. Thermodynamic Cycle for the Formation of Soddyite $(UO_2)_2(SiO_4)\cdot 2H_2O$ from Oxides and Elements

soddyite $(UO_2)_2(SiO_4)\cdot 2H_2O$	
$(UO_2)_2(SiO_4)\cdot 2H_2O$ xl, 25 °C = $2UO_3$ sln,702 °C + SiO_2 sln,cr, 702 °C + $2H_2O$ g, 702 °C	$\Delta H1 = \Delta H_{ds\ soddyite}$
UO_3 xl, 25 °C = UO_3 sln,702 °C	$\Delta H2 = \Delta H_{ds}(UO_3)$
SiO_2 xl, cr, 25 °C = SiO_2 sln,702 °C	$\Delta H3 = \Delta H_{ds}(SiO_2)$
H_2O l, 25 °C = H_2O g, 702 °C	$\Delta H4 = \Delta H_{ds}(H_2O)$
$2UO_3$ xl, 25 °C + SiO_2 xl, 25 °C + 2 H_2O l, 25 °C = $(UO_2)_2(SiO_4)\cdot 2H_2O$ xl, 25 °C	$\Delta H5 = \Delta H_{f,\ ox} = -\Delta H1 + 2\Delta H2 + \Delta H3 + 2\Delta H4$
U xl, 25 °C + 3/2 O_2 g, 25 °C = UO_3 xl, 25 °C	$\Delta H6 = \Delta H_f\ UO_3$
Si xl, 25 °C + O_2 g, 25 °C = SiO_2 xl, cr, 25 °C	$\Delta H7 = \Delta H_f\ SiO_2$
H_2 g, 25 °C + 1/2 O_2 g, 25 °C = H_2O l, 25 °C	$\Delta H8 = \Delta H_f\ H_2O$
2U xl, 25 °C + Si xl, 25 °C + $2H_2$ g, 25 °C + $5O_2$ g, 25 °C = $(UO_2)_2(SiO_4)\cdot 2H_2O$ xl, 25 °C	$\Delta H9 = \Delta H_{fr\ el} = \Delta H5 + 2\Delta H6 + \Delta H7 + 2\Delta H8$

To facilitate dissolution of materials and also maintain the oxidative atmosphere, oxygen gas is constantly bubbled through the solvent. Change of the solvent color to bright yellow indicates that the uranium and molybdenum remain in their initial +6 oxidation state during the measurements. Structural water and carbonate anions vaporize and are expelled from the calorimeter by the flowing gas. The final state is well-defined: dissolved U^{6+} and other cationic and anionic species, with evolved H_2O and CO_2. The solutes are present at low concentration so dilution effects need not be considered, and the solution enthalpy does not depend on the amount dissolved or the presence of other solutes.

Table 1 summarizes formation enthalpies for uranyl minerals at room temperature collected via high temperature solution calorimetry.[31−34] We report enthalpies of formation from elements and from corresponding oxides. The latter better illustrate energetic trends among the different minerals, since the enthalpies of formation of constituent oxides, which obscure any small differences in energetics, are not included in calculations. All values are normalized per one uranyl unit per formula for easier comparison.

The general structural motif of most uranyl minerals is two-dimensional uranyl polyhedra-based sheets with cations and/or water molecules separating the layers (Figure 1).[15] However for each class of materials, layers have different topology. A few minerals deviate from this trend and possess one- or three-dimensional structures. Therefore energetics of uranyl oxides, carbonates, phosphates, and silicates are difficult to compare directly based only on structural considerations. However, we are able to evaluate the contribution of acid−base interactions to the energetics within each class of materials.

Two types of Lewis acid−base interactions can be separated. First, minerals become more stable relative to oxides as acidity of anions increases in the order $OH^- < SiO_4^{4-} < CO_3^{2-} < PO_4^{3-}$ and interaction between uranyl cations and those anions becomes more exothermic. Reactions 1−4 demonstrate the relative energetic trend of Lewis interactions for the case of CaO.

$$CaO + H_2O = Ca(OH)_2 \quad \Delta H = -97.2 \pm 1.6\ \text{kJ/mol} \tag{1}$$

$$CaO + 0.5\ SiO_2 = 0.5Ca_2SiO_4 \quad \Delta H = -102.1 \pm 2.0\ \text{kJ/mol} \tag{2}$$

$$CaO + CO_2 = CaCO_3 \quad \Delta H = -210.8 \pm 1.9\ \text{kJ/mol} \tag{3}$$

$$CaO + 1/3P_2O_5 = 1/3Ca_3(PO_4)_2 \quad \Delta H = -268.9 \pm 5.1\ \text{kJ/mol} \tag{4}$$

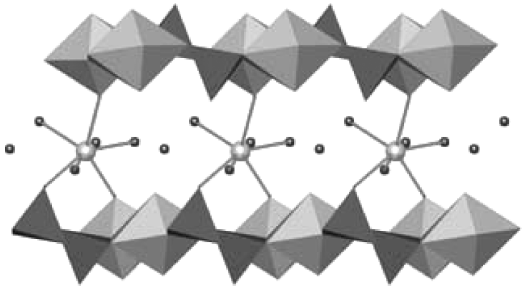

Figure 1. Polyhedral representation of the layered crystal structure of uranophane along the projection of uranyl silicate layers separated by Ca^{2+} cations and water molecules.[11] Lighter polyhedra correspond to uranyl units, darker correspond to silicates; spheres between the layers are Ca^{2+} cations (larger) and water molecules (smaller). Copied from ref 11 with permission.

Due to the higher acidity of UO_3 compared to CaO, energetics of interaction of UO_3 with the same acidic oxides as in eqs 1−4 is significantly less exothermic but should follow a similar trend: uranyl phosphates would be the most stable minerals, followed by carbonates, silicates, and then oxides. However, within each class of uranyl materials, enthalpy of formation from oxides is additionally influenced by the interactions between a particular acidic oxide and basic oxide related to cations located between the uranyl sheets.

The most energetically favorable phases are grimselite $K_3NaUO_2(CO_3)_3(H_2O)$ and andersonite $Na_2Ca[(UO_2)(CO_3)_3](H_2O)_5$, both with zero-dimensional structures consisting of isolated uranyl clusters surrounded by carbonate triangles.[31] The strong interaction between four basic interlayer cations K^+ and Na^+ (the highest alkali content among all studied materials) with a relatively strong acid, CO_3^{2-}, leads to strongly negative formation enthalpies from oxides equal to −989.3 ± 14.0 kJ/mol. Andersonite $Na_2Ca[(UO_2)(CO_3)_3](H_2O)_5$ contains two Na^+ and one less basic Ca^{2+}, thus its enthalpy of formation, −710.4 ± 9.1 kJ/mol, is more positive than that of grimselite. Enthalpy of formation of rutherfordine UO_2CO_3 with layered structure of uranyl hexagons and carbonate triangles, where no interlayer cations are involved, −99.1 ± 4.2 kJ/mol, reflects only the uranyl−carbonate acid−base energetic contribution, and is less exothermic than values for grimselite and andersonite.[31]

Uranyl phosphate, $UO_2(PO_4)_{2/3}(H_2O)_{4/3}$, also consists of only electro-neutral layers. However, the different topology of the layers, stronger uranyl−phosphate interactions compared to uranyl−carbonate, and the exothermic contribution of water

dx.doi.org/10.1021/ie2002582 |Ind. Eng. Chem. Res. 2012, 51, 607–613

incorporation result in a more exothermic enthalpy of formation, −227.2 ± 2.3 kJ/mol, compared to rutherfordine.[34] Another reported uranyl phosphate $UO_2HPO_4(H_2O)_3$ also does not incorporate any cations into the structure and thus has a smaller Lewis contribution to the formation enthalpy. Its uranyl phosphate layers have the same autunite topology as in $UO_2(PO_4)_{2/3}(H_2O)_{4/3}$, but are in turn connected by uranyl pentagonal bipyramids into a framework structure. The formation of this more rigid structure is the reason for more exothermic formation enthalpy, −241.0 ± 3.9 kJ/mol, compared to layered $UO_2HPO_4\ (H_2O)_3$.[34]

The formation of uranyl silicates from oxides is less favorable than for phosphates despite the presence of one alkaline (or 0.5 alkaline earth) cation per formula unit. Also partial protonation of the terminal oxygen in the silicate group makes $HSiO_4^{3-}$ less acidic compared to PO_4^{3-} and CO_3^{2-}.

Na−boltwoodite $Na(UO_2)(HSiO_4)(H_2O)$, boltwoodite $K(UO_2)(HSiO_4)(H_2O)$, and uranophane $Ca_{1/2}(UO_2)(HSiO_4)\cdot 2.5H_2O$ are layered materials. Their negatively charged uranyl silicate sheets, consisting of edge-sharing uranyl pentagonal bipyramids and silicate tetrahedra, are counter-balanced by interlayer K^+, Na^+, or Ca^{2+} cations.[37] Water molecules are located between the layers. Thus, acid−base interactions between cation oxides, CaO, Na_2O, or K_2O, and silicate anions become more exothermic with decreasing acidity of cation oxides. Le et al.[38,39] have shown that the enthalpies of formation from constituent oxides for cobalt phosphate salts (where Na^+, K^+, and Rb^+ are also present as interlayer cations) change linearly with acidity of alkali oxides. These linear relationships are shown in Figure 2 where oxide acidity is expressed in the Smith scale.[40] Enthalpies of formation of boltwoodite, Na-boltwoodite, and uranophane from oxides are also plotted in Figure 2 as a function of oxide acidity and show linear trends with the strongest contribution from K_2O.[41] The different slopes of the fitting lines for cobalt phosphate and uranyl silicate salts reflect much more exothermic interactions in the $CoO-P_2O_5$ group compared to UO_3-SiO_2 oxides. This observation is consistent with the energetic trends we found.

The structure of soddyite $(UO_2)(SiO_4)_{1/2}(H_2O)$, the least energetically favorable uranyl silicate, is based on chains of the same topology as in boltwoodites and uranophane, except that these chains in turn are joined into the three-dimensional structure by uranyl pentagonal bipyramids.[42] Apparently, the formation of denser framework structure does not lend any special stability to the mineral compared to layered materials.[33]

Uranyl oxide hydrates have the least exothermic enthalpies of formation from oxides. Isostructural Na−compregnacite $Na_{0..34}(UO_2)O_{0.67}(OH)(H_2O)_{1.2}$ and becquerelite $Ca_{0.17}(UO_2)\ O_{0.67}(OH)\ (H_2O)_{1.3}$ consist of uranyl hydroxide chains with the same structural motif as in boltwoodite and uranophane.[15] Similar chains are connected to layers by silicate tetrahedra in boltwoodite and uranophane or by uranyl pentagonal bipyramids in compregnacite and becquerelite. Negatively charged layers are separated by Na^+ and Ca^{2+} cations. Such structural arrangement rules out any other than Lewis interactions between basic cations and adjacent layers. Based on this observation, we suggest similar linear trend for formation enthalpies of isostructural uranyl oxides hydrates as function of acidity of interlayer cations as for uranyl silicates. The data are shown in Figure 2. Extrapolating linear enthalpy trend to the K^+, as shown by the dashed line, we predict enthalpy of formation for the compregnacite $Na_{0..34}(UO_2)O_{0.67}(OH)(H_2O)_{1.2}$ from UO_3, H_2O and K_2O as −58 kJ/mol (or −348 kJ/mol for $Na_2[(UO_2)_3O_2(OH)_3]_2\cdot 7H_2O$).

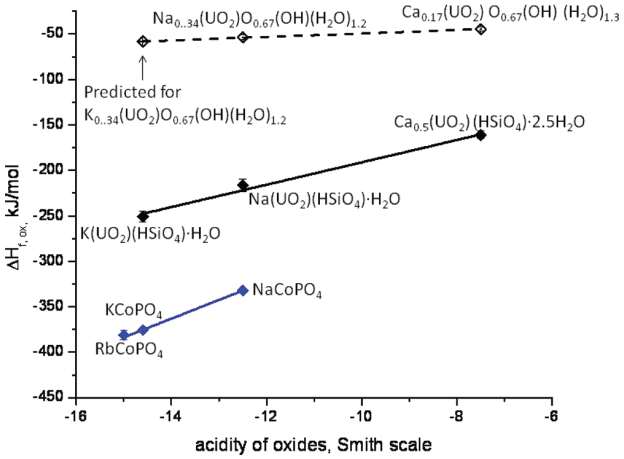

Figure 2. Enthalpies of formation from oxides for uranyl silicate, uranyl oxide hydrate, and cobalt phosphate salts as a function of acidity of alkali and alkali-earth oxides.[40]

Enthalpies of formation from oxides permit calculations of formation enthalpies from elements under standard conditions (temperature 25 °C and pressure 1 bar) for all materials (Table 2). Combined with solubility results and hence standard Gibbs free energies of formation, these data directly yield entropies of each phase of interest. Therefore, the combination of calorimetry and solubility measurements represents a powerful approach for fully characterizing the thermodynamic properties of uranyl minerals.

Solubility Measurements. In our solubility studies,[33,34,41] measurements were conducted primarily under the low pH conditions at which UO_2^{2+} is the dominant aqueous uranyl species. This approach eliminates the need to rely on knowledge of the thermodynamic properties of the aqueous uranyl species that exist under higher pH conditions, and thereby improves the accuracy of the thermodynamic calculations. Successful extraction of thermodynamic data from solubility measurements requires a range of measurements or controls on the experimental systems: (1) rigorous demonstration of the attainment of equilibrium through solubility reversals; (2) measurements of the equilibrium pH and the total aqueous equilibrium concentrations of all mineral-forming cations in the system, allowing for the calculation of the speciation of all of the cations in solution; (3) ionic strength control or measurement; and (4) determination that secondary mineral phases do not form during experimentation.

In a typical solubility experiment, synthesized uranyl mineral powder was placed in contact with a fixed ionic strength solution, and the pH of the suspension was adjusted to a desired value using concentrated acid or base. Ionic strength was buffered using $NaClO_4$. Shorter dissolution times or oversaturation of the experimental solutions were achieved by spiking the initial aqueous phase with dissolved uranium and other mineral-forming cations. Solubility experiments of uranyl silicates involved introduction of silica gel into the experimental systems to buffer aqueous Si concentrations and to ensure rapid attainment of equilibrium with respect to dissolved Si. The experimental solutions were agitated, and the aqueous phase was sampled repeatedly as a function of time until steady-state conditions were attained. These samples were then analyzed for dissolved total metal concentrations, using inductively coupled plasma optical emission spectroscopy (ICP-OES). The solid phases were

characterized by powder X-ray diffraction and by FTIR-ATR spectrometry both before and after the experiments to check for phase stability under the experimental conditions. The ATR permitted collection of IR spectra for sample areas as small as 12 μm,[2] and was used to systematically search for impurity phases that may not have been detected by XRD.

As an example, the equilibrium constant for the dissolution reaction of soddyite

$$4H^+ + (UO_2)_2(SiO_4)(H_2O)_{2(\text{soddyite})} = 2UO_2^{2+} + H_4SiO_4 + 2H_2O \quad (5)$$

can be expressed as

$$K_{(1)} = \frac{a^2UO_2^{+2} * a_{H_4SiO_4}}{a^4H^+} \quad (6)$$

,where a represents the activity of the subscripted aqueous species. For experiments conducted below pH 5 where UO_2^{2+} and H_4SiO_4 species dominate the total dissolved uranium and silica budgets, respectively, the value of $K_{(1)}$ can be directly measured by determining the equilibrium pH and concentrations of UO_2^{2+} and H_4SiO_4. Standard states for minerals and for H_2O are defined to be the pure phases at the pressure and temperature of interest, and the standard state for aqueous species is defined to be a hypothetical one molal solution that behaves as if it is infinitely dilute. Because we buffer the ionic strength with a relatively inert background electrolyte such as $NaClO_4$, we can convert the measured molality of UO_2^{2+} to an activity using the extended Debye−Hückel equation.[33] The activity of H^+ is directly determined through pH measurements.

The equilibrium constant directly yields a value for the change in standard state Gibbs free energy for the reaction, $\Delta G^\circ_{\text{reaction}}$:

$$\log K_{(1)} = \frac{-\Delta G^\circ_{\text{reaction}}}{2.303RT} \quad (7)$$

where R and T represent the gas constant and absolute temperature, respectively.

The parameter $\Delta G^\circ_{\text{reaction}}$ is defined as follows:

$$\Delta G^\circ_{\text{reaction}} = 2\Delta G^\circ_{f(UO_2^{+2})} + \Delta G^\circ_{f(H_4SiO_4)} + 2\Delta G^\circ_{f(H_2O)} - 4\Delta G^\circ_{f(H^+)} - \Delta G^\circ_{f(\text{Soddyite})} \quad (8)$$

where $\Delta G^\circ_{f(i)}$ represents the standard Gibbs free energy of formation at room temperature for the species in the parentheses. Because the values of $\Delta G^\circ_{f(i)}$ are well-established for liquid H_2O and for all of the major aqueous species, the experimental determination of $\Delta G^\circ_{\text{reaction}}$ enables us to calculate $\Delta G^\circ_{\text{f (Soddyite)}}$ directly. Standard Gibbs free energies of formation for other uranyl minerals, obtained in an approach similar to that described for soddyite, under standard state, are summarized in Table 1.

Although in theory only one solubility measurement, conducted at a single ionic strength, is sufficient to determine the value of $K_{(1)}$, significant improvement in the uncertainty associated with these values is obtained by conducting the solubility measurements both as a function of pH and as a function of ionic strength. The measurements conducted as a function of pH not only provide additional constraints on the thermodynamic values, but they also constrain the stoichiometry of the dissolution reaction. Because reaction 5 depends on pH, a fixed relationship exists between the extent of dissolution in terms of the uranyl concentration and solution pH. Thus, the solubility measurements conducted as a function of pH enable us to determine whether such a relationship exists.

Although the direct determination of uranyl mineral solubilities is of use, the extraction of standard Gibbs free energies of formation from solubilities is perhaps of greater importance in modeling uranyl mineral stabilities and solubilities under conditions not directly studied in the laboratory. The calculated Gibbs free energy values can be used to determine relative stabilities of uranyl minerals under a wide range of conditions of environmental and geological interest. The Gibbs free energy values can also be used to calculate equilibrium constant values for any reaction involving the studied uranyl mineral phases, enabling estimation of the solubility of any mineral assemblage for different conditions. Because it is impossible to measure uranium concentrations in equilibrium with all uranyl phases under all conditions in the laboratory, it is crucial to be able to estimate these concentrations in order to assess the mobility of uranium in systems not directly studied in the laboratory. The thermodynamic properties that we determined enable such extrapolation.

Environmental Applications. Groundwater, where uranyl minerals precipitate, is typically rich in silica, carbonate, and Ca^{2+},[43] thus the stability diagram for $CaO-SiO_2-UO_3-H_2O$ system is of great importance. A number of diagrams have been previously reported. Finch and Ewing[1] calculated an activity−activity diagram based on the data from solubility measurements at undersaturated conditions with the stability field of becquerelite suggested from petrographic results. Prikryl[43] developed the three-dimensional Log $[UO_2^{2+}/(H^+)^2]$ vs Log $[(Ca^{2+})/(H^+)^2]$ vs Log $[SiO_2(aq)]$ diagram for uranophane using measured solubility data. Also Murphy[44] have shown the stability of uranophane over the range of different conditions. Diagrams of Finch[29] and Chen et al.[30] are based exclusively on predicted Gibbs free energies of formation. The thermodynamic data set in this manuscript allows the calculation of stability fields for selected uranyl minerals and it enables us to determine the accuracy of previously predicted values. Figure 3 shows the log $(a(Ca^{2+})/[a(H^+)^2 - \log a(H_4SiO_4])$ diagram for uranyl oxides and silicates. Stability fields recommended by Finch and Ewing[1] as well as predicted by Chen et al.[30] are also shown. Predicted values from Finch[29] are analyzed in detail by Chen et al.[30] and therefore are not marked.

The diagram (Figure 3) confirms the conclusions of Chen et al.[30] and mineral stability relationships observed in nature. Metaschoepite is a metastable phase that is replaced by uranyl silicates if silica is dissolved in groundwater in any significant amount. Stability of metaschoepite is limited to lower Si concentrations compared to that calculated by Chen et al.,[30] thus explaining the favorable formation of soddyite for all groundwater compositions at the low Ca^{2+} contents assumed by Chen et al. Soddyite and uranophane are the most abundant minerals that form in contact with groundwater of almost any composition. Becquerelite is stable under more acidic conditions and low silica concentration, but can coexist with soddyite and uranophane; there are certain, but rare reports of groundwater with chemistry favorable for such formations.[45] A few other uranyl silicates, such as weeksite, are known to occur

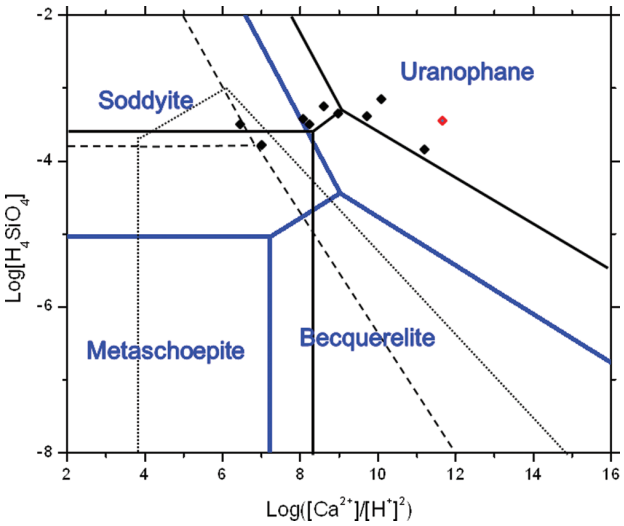

Figure 3. Stability fields of minerals in the $CaO-SiO_2-UO_3-H_2O$ system. Stability fields based on experimental results are indicated by blue lines. Stability fields predicted by Chen et al.[30] are shown as solid lines. Stability fields derived by Finch and Ewing[1] are shown in dashed lines with stability of becquerelite (dotted line) estimated from petrographic data.[1] Black points and red point are composition of groundwater and the composition of J-13 water, respectively, taken from Chen et al.[30]

naturally and thermodynamic data for these minerals need to be determined.

There are not enough solubility data for uranyl carbonates to revise their stability diagram. However, relationships between metaschoepite and becquerelite found for the $CaO-SiO_2-UO_3-H_2O$ system will also extend to $CaO-CO_2-UO_3-H_2O$. Given that metaschoepite stability is limited to log $(a(Ca^{2+})/a(H^+)^2) = 7.2$, becquerelite formation becomes favorable for almost all groundwater compositions shown by Chen et al.[30]

Uranyl phosphates have the lowest solubilities of the uranyl minerals studied and thus their stability and favorable formation conditions are critical. $UO_2HPO_4 \cdot 3H_2O$ can be formed according to:

$$H^+ + (UO_2)_3(PO_4)_2 \cdot 4H_2O = UO_2HPO_4 \cdot 3H_2O + 2UO_2^{2+} + PO_4^{3-} + H_2O \quad (9)$$

and therefore its formation depends on pH, UO_2^{2+}, and PO_4^{3-} activities. At pH values lower than 4, $(UO_2)_3(PO_4)_2 \cdot 4H_2O$ is stable at any uranyl cation activities above 10^{-13}. If pH values are above 5, $UO_2HPO_4 \cdot 3H_2O$ can become the more stable phase due to formation of uranyl aqueous complexes and, as a result, significant decrease of UO_2^{2+} activity. When Ca^{2+} is present, $Ca(UO_2)_2(PO_4)_2 \cdot 3H_2O$ can form according to the reaction

$$(UO_2)_3(PO_4)_2 \cdot 4H_2O + Ca^{2+} = UO_2^{2+} + H_2O + Ca(UO_2)_2(PO_4)_2 \cdot 3H_2O \quad (10)$$

but only if the activity of Ca^{2+} is considerably larger (more than an order of magnitude) than the activity of UO_2^{2+}. Thus, $(UO_2)_3(PO_4)_2 \cdot 4H_2O$ is more stable than $Ca(UO_2)_2(PO_4)_2 \cdot 3H_2O$ in Ca^{2+}-rich waters only if they are highly contaminated with uranium.

CONCLUSIONS

The experimental data summarized here yield an internally consistent set of thermodynamic properties for a wide range of environmentally important uranyl minerals. Although the thermodynamic properties of only some of the most geologically and environmentally important and abundant uranyl phases have been determined, the creation of this database represents a crucial first step toward quantitative assessment of uranium mobility in oxidized geologic systems. These thermodynamic data can be used not only to determine the concentration of uranium that exists in equilibrium with secondary uranyl minerals in groundwater, or ore-weathering, or spent nuclear fuel repository systems, but also to determine which of these phases are the most stable under a wide range of conditions of geologic and environmental interest. The quality and extent of the thermodynamic data set for uranyl phases have significantly improved over the past few years, but much experimental work remains to be done. In particular, experimental studies of uranyl silicates need to be expanded, and solubilities of uranyl carbonates must be included in the data set as well. All studies to date have involved pure end-member uranyl phases, but incorporation of other elements into these phases may lead to nonideal behavior that affects mineral stabilities and solubilities, and these effects must be quantified as well. In general, the accuracy of models of the fate and transport of uranium in environmental and geologic systems is only as good as the thermodynamic data set that forms its foundation. This data set has vastly grown over the past decade but still is incomplete, and more research is needed to yield a complete understanding of the behavior of uranium in oxidizing systems.

AUTHOR INFORMATION

Corresponding Author

*E-mail: anavrotsky@ucdavis.edu.

ACKNOWLEDGMENT

Funding for the initial stages of this project was provided by a U.S. Department of Energy, Office of Science and Technology and International (OST&I) grant under the Source Term Thrust program. Further material is based upon work supported as part of the Materials Science of Actinides, an Energy Frontier Research Center funded by the U.S. Department of Energy, Office of Science, Office of Basic Energy Sciences under Award DE-SC0001089.

REFERENCES

(1) Finch, R. J.; Ewing, R. C. The Corrosion of Uraninite under Oxidizing Conditions. *J. Nucl. Mater.* **1992**, *190*, 133–156.

(2) Wronkiewicz, D. J.; Bates, J. K.; Gerding, T. J.; Veleckis, E.; Tani, B. S. Uranium release and secondary phase formation during unsaturated testing of uranium dioxide at 90 °C. *J. Nucl. Mater.* **1992**, *190*, 107–27.

(3) Wronkiewicz, D. J.; Bates, J. K.; Wolf, S. F.; Buck, E. C. Ten-year results from unsaturated drip tests with UO_2 at 90°: Implications for the corrosion of spent nuclear fuel. *J. Nucl. Mater.* **1996**, *238* (1, Spent Fuels), 78–95.

(4) Pearcy, E. C.; Prikryl, J. D.; Murphy, W. M.; Leslie, B. W. Alteration of uraninite from the Nopal I deposit, Pena Blanca District, Chihuahua, Mexico, compared to degradation of spent nuclear fuel in the proposed U.S. high-level nuclear waste repository at Yucca Mountain, Nevada. *Appl. Geochem.* **1994**, *9* (6), 713–32.

(5) Finch, R. J.; Ewing, R. C. Alteration of natural uranium dioxide under oxidizing conditions from Shinkolobwe, Katanga, Zaire: A natural analog for the corrosion of spent fuel. *Radiochim. Acta* **1991**, *52*−*53* (Pt. 2), 395–401.

(6) Isobe, H.; Murakami, T.; Ewing, R. C. Alteration of uranium minerals in the Koongarra deposit, Australia: Unweathered zone. *J. Nucl. Mater.* **1992**, *190*, 174–87.

(7) Bates, J. K.; Tani, B. S.; Veleckis, E.; Wronkiewicz, D. J. Identification of secondary phases formed during unsaturated reaction of uranium dioxide with EJ-13 water. *Mater. Res. Soc. Symp. Proc.* **1990**, *176* (Sci. Basis Nucl. Waste Manage. 13), 499–506.

(8) Fattahi, M.; Guillaumont, R. Determination of the concentration of uranium(IV) and uranium(VI) in anoxic leaching solutions of uranium dioxide. *Radiochim. Acta* **1993**, *61* (3−4), 155–62.

(9) Burns, P. C.; Ewing, R. C.; Miller, M. L. Incorporation mechanisms of actinide elements into the structures of U^{6+} phases formed during the oxidation of spent nuclear fuel. *J. Nucl. Mater.* **1997**, *245* (1), 1–9.

(10) Douglas, M.; Clark, S. B.; Friese, J. I.; Arey, B. W.; Buck, E. C.; Hanson, B. D. Neptunium(V) Partitioning to Uranium(VI) Oxide and Peroxide Solids. *Environ. Sci. Technol.* **2005**, *39* (11), 4117–4124.

(11) Klingensmith, A. L.; Burns, P. C. Neptunium substitution in synthetic uranophane and soddyite. *Am. Mineral.* **2007**, *92* (11−12), 1946–1951.

(12) Shuller, L. C.; Ewing, R. C.; Becker, U. Quantum-mechanical evaluation of Np-incorporation into studtite. *Am. Mineral.* **2010**, *95* (8−9), 1151–1160.

(13) Grenthe, I.; Wanner, H.; Forest, I. OECD Nuclear Energy Agency. *Chemical Thermodynamics of Uranium*; Elsevier Science Pub. Co.: Amsterdam, New York, 1992; p xvii, 715 pp.

(14) Guillaumont, R., Ed. *Update on the Chemical Thermodynamics of Uranium, Neptunium, Plutonium, Americium and Technetium*; Elsevier Science: New York, 2003; 964 pp.

(15) Burns, P. C. U^{6+} minerals and inorganic compounds: insights into an expanded structural hierarchy of crystal structures. *Can. Mineral.* **2005**, *43* (6), 1839–1894.

(16) Santalova, N. A.; Vidavskii, L. M.; Dunaeva, K. M.; Ippolitova, E. A. Enthalpy of formation of uranium trioxide dihydrate. *Radiokhimiya* **1971**, *13* (4), 592–7.

(17) Tasker, I. R.; O'Hare, P. A. G.; Lewis, B. M.; Johnson, G. K.; Cordfunke, E. H. P. Thermochemistry of uranium compounds. XVI. Calorimetric determination of the standard molar enthalpy of formation at 298.15 K, low-temperature heat capacity, and high-temperature enthalpy increments of $UO_2(OH)_2.H_2O$ (schoepite). *Can. J. Chem.* **1988**, *66* (4), 620–5.

(18) Bruno, J.; Sandino, A. The solubility of amorphous and crystalline schoepite in neutral to alkaline aqueous solutions. *Mater. Res. Soc. Symp. Proc.* **1989**, *127* (Sci. Basis Nucl. Waste Manag. 12), 871–8.

(19) Kramer-Schnabel, U.; Bischoff, H.; Xi, R. H.; Marx, G. Solubility products and complex formation equilibria in the systems uranyl hydroxide and uranyl carbonate at 25 °C and I = 0.1M. *Radiochim. Acta* **1992**, *56* (4), 183–8.

(20) Meinrath, G.; Kimura, T. Behavior of uranium (VI) solids under conditions of natural aquatic systems. *Inorg. Chim. Acta* **1993**, *204* (1), 79–85.

(21) Giammar, D. E.; Hering, J. G. Influence of Dissolved Sodium and Cesium on Uranyl Oxide Hydrate Solubility. *Environ. Sci. Technol.* **2004**, *38* (1), 171–179.

(22) Gorman-Lewis, D.; Burns, P. C.; Fein, J. B. Review of uranyl mineral solubility measurements. *J. Chem. Thermodyn.* **2008**, *40* (3), 335–352.

(23) Sergeeva, E. I.; Nikitin, A. A.; Khodakovskii, I. L.; Naumov, G. B. Equilibriums in the uranium trioxide-carbon dioxide-water system at 25−200°. *Geokhimiya* **1972**, *11*, 1340–50.

(24) Meinrath, G.; Kato, Y.; Kimura, T.; Yoshida, Z. Solid-aqueous phase equilibria of uranium(VI) under ambient conditions. *Radiochim. Acta* **1996**, *75* (3), 159–167.

(25) Cordfunke, E. H. P.; O'Hare, P. A. G. *The Chemical Thermodynamics of Actinide Elements and Compounds, Pt. 3: Miscellaneous Actinide Compounds*; IAEA: Vienna, 1978; 85 pp.

(26) Alwan, A. K.; Williams, P. A. The aqueous chemistry of uranium minerals. 2. Minerals of the liebigite group. *Mineral. Mag.* **1980**, *43* (329), 665–7.

(27) Cordfunke, E. H. P.; Ouweltjes, W. Standard enthalpies of formation of uranium compounds. XII. Anhydrous phosphates. *J. Chem. Thermodyn.* **1985**, *17* (5), 465–71.

(28) Barten, H. The thermochemistry of uranyl phosphates. *Thermochim. Acta* **1988**, *126*, 375–83.

(29) Finch, R. J. Thermodynamic stabilities of U(VI) minerals: estimated and observed relationships. *Mater. Res. Soc. Symp. Proc.* **1997**, *465* (Scientific Basis for Nuclear Waste Management XX), 1185–1192.

(30) Chen, F.; Ewing, R. C.; Clark, S. B. The Gibbs free energies and enthalpies of formation of U^{6+} phases: An empirical method of prediction. *Am. Mineral.* **1999**, *84* (4), 650–664.

(31) Kubatko, K.-A.; Helean, K. B.; Navrotsky, A.; Burns, P. C. Thermodynamics of uranyl minerals: Enthalpies of formation of rutherfordine, UO_2CO_3, andersonite, $Na_2CaUO_2(CO_3)_3(H_2O)_5$, and grimselite, $K_3NaUO_2(CO_3)_3H_2O$. *Am. Mineral.* **2005**, *90* (8−9), 1284–1290.

(32) Kubatko, K.-A.; Helean, K.; Navrotsky, A.; Burns, P. C. Thermodynamics of uranyl minerals: Enthalpies of formation of uranyl oxide hydrates. *Am. Mineral.* **2006**, *91* (4), 658–666.

(33) Gorman-Lewis, D.; Mazeina, L.; Fein, J. B.; Szymanowski, J. E. S.; Burns, P. C.; Navrotsky, A. Thermodynamic properties of soddyite from solubility and calorimetry measurements. *J. Chem. Thermodyn.* **2007**, *39* (4), 568–575.

(34) Gorman-Lewis, D.; Shvareva, T.; Kubatko, K.-A.; Burns, P. C.; Wellman, D. M.; McNamara, B.; Szymanowski, J. E. S.; Navrotsky, A.; Fein, J. B. Thermodynamic Properties of Autunite, Uranyl Hydrogen Phosphate, and Uranyl Orthophosphate from Solubility and Calorimetric Measurements. *Environ. Sci. Technol.* **2009**, *43* (19), 7416–7422.

(35) Navrotsky, A. Progress and New Directions in High-Temperature Calorimetry. *Phys. Chem. Miner.* **1977**, *2* (1−2), 89–104.

(36) Navrotsky, A. Progress and new directions in high temperature calorimetry revisited. *Phys. Chem. Miner.* **1997**, *24* (3), 222–241.

(37) Burns, P. C. The structure of boltwoodite and implications of solid solution toward sodium boltwoodite. *Can. Mineral.* **1998**, *36* (4), 1069–1075.

(38) Le, S.-N.; Navrotsky, A. Energetics of phosphate frameworks containing zinc and cobalt: $NaZnPO_4$, $NaH(ZnPO_4)_2$, $NaZnPO_4 \cdot H_2O$, $NaZnPO_4 \cdot 4/3H_2O$, and $NaCo_xZn_{1-x}PO_4 \cdot 4/3H_2O$. *J. Solid State Chem.* **2007**, *180* (9), 2443–2451.

(39) Le, S.-N.; Navrotsky, A. Energetics of formation of alkali and ammonium cobalt and zinc phosphate frameworks. *J. Solid State Chem.* **2008**, *181* (1), 20–29.

(40) Smith, D. W. An acidity scale for binary oxides. *J. Chem. Educ.* **1987**, *64* (6), 480–1.

(41) Shvareva, T.; Mazeina, L.; Gorman-Lewis, D.; Burns, P. C.; Szymanowski, J. E. S.; Fein, J. B.; Navrotsky, A. Thermodynamic Characterization of Boltwoodite and Uranophane: Enthalpy of Formation and Aqueous Solubility. *Geochim. Cosmochim. Acta* **2011**, *75* (18), 5269–5282.

(42) Demartin, F.; Gramaccioli, C. M.; Pilati, T. The importance of accurate crystal structure determination of uranium minerals. II. Soddyite $(UO_2)_2(SiO_4) \cdot 2H_2O$. *Acta Crystallogr., Sect. C: Cryst. Struct. Commun.* **1992**, *C48* (1), 1–4.

(43) Prikryl, J. D. Uranophane dissolution and growth in $CaCl_2$−SiO_2(aq) test solution. *Geochim. Cosmochim. Acta* **2008**, *72*, 4508–4520.

(44) Murphy, W. M. Hydrothermal phase relations among uranyl minerals at the Nopal I analog site. *Mater. Res. Soc. Symp. Proc.* **2007**, *985* (Sci. Basis Nucl. Waste Manage., 30), 53–58.

(45) Faust, S. D.; Aly, O. M. *Chemistry of Natural Waters*; Ann Arbor Science Publishers: Ann Arbor, MI, 1981; 416 pp.